Title : **Development of a Mechanically Stable Human Hair Keratin Film for Cell Culture**

Authors : Bee Yi Tan,[1] Luong T. H. Nguyen,[2] Kee Woei Ng[1,3,4,*]

[1] School of Materials Science and Engineering, Nanyang Technological University, 50 Nanyang Avenue, 639798, Singapore

[2] William G. Lowrie Department of Chemical and Biomolecular Engineering, The Ohio State University, Columbus, Ohio 43210, USA

[3] Center for Nanotechnology and Nanotoxicology, Harvard T.H. Chan School of Public Health, Harvard University, 665 Huntington Avenue, Boston, Massachusetts 02115, USA

[4] Environmental Chemistry and Materials Centre, Nanyang Environment and Water Research Institute, Nanyang Technological University, 1 Cleantech Loop, CleanTech One, 637141, Singapore

[*] Corresponding author. E-mail address: kwng@ntu.edu.sg

Keywords: human hair, keratins, protein film, stretchable, cell carrier

Abstract

An easy-to-handle keratin film was successfully fabricated using solely purified hair keratins. Keratin was extracted from human hair by an existing protocol. The extracted keratin was made into a mechanically stable film by solution casting and air-drying at room temperature. The films obtained were characterized for surface morphology, wettability, protein secondary structures, mechanical properties, permeability, and thermal properties. Interestingly, the keratin film showed distinct surface and cross-sectional morphology, and protein secondary structure transformation. In addition, the keratin film exhibited Young's modulus of 1.05 ± 0.09 GPa when it was dry. In the wet state, the keratin film behaved as viscoelastic material and was highly stretchable at 179 ± 17 % strain at break. Permeability test was conducted using 20 kDa-FITC dextran which revealed an anomalous diffusion mechanism through the keratin film. Additionally, the keratin film elicited positive cellular responses by human epidermal keratinocytes (HEKs) in terms of enhanced cell proliferation, viability, keratin 14 expression, and IL-1α secretion, in comparison to collagen I. Taken together, a human hair keratin-based film with its mechanical and thermal stability, and cytocompatibility, presents a promising platform for cell culture applications.

1. Introduction

Naturally derived biomaterials have been extensively studied as they are generally perceived as being more sustainable and relevant for clinically viable therapies when compared to synthetic biomaterials [1]. However, issues related to foreign-body immunogenic reactions, pathogens, and potential conflicts with cultural and religious beliefs may arise if these are of

---

Abbreviations:
HEKs, human epidermal keratinocytes
KAP, keratin-associated proteins
THP, total hair proteins.

animal origins [2]. Therefore, human-derived biomaterials have received more attention as the next generation of regenerative biomaterials. Human hair keratins are leading contenders after decades of optimization in terms of extraction, purification, and characterization [3, 4]. In addition, human hair proteins can also potentially minimize the risk of immunological rejection compared to animal-derived biomaterials, especially when autologous sources are used [5]. This encourages greater patient acceptance and compliance while reducing the chances of interspecies and blood-borne pathogen transfers.

Human hair proteins consist of two main components: Keratins and keratin-associated proteins (KAP). The human hair keratin family consists of 11 acidic subtypes with molecular weight 40-55 kDa and 6 basic subtypes with molecular weight 55-65 kDa [6-8]. Keratins have been found to support cell attachment due to the presence of cell recognition sites such as leucine-aspartic acid-valine (LDV) and glutamic acid–aspartic acid-serine (EDS) [9]. Keratins exhibit unique ability to assemble in a hierarchical manner starting from dimerization, leading to the final 10 nm intermediate filament product; the possibility for this to happen with hair keratins was demonstrated recently [10].

Because of the presence of multiple functional groups, in particular thiols, keratins can also interact with each other in a non self-assembly manner to produce various forms such as hydrogels [11, 12], sponges [13, 14], fibrous matrices [15], thin films [16, 17], and coatings [18, 19]. KAP is a matrix protein that is even more abundant in cysteines. KAP thus acts as natural crosslinkers to facilitate disulfide bonding, providing a tough and durable structure to withstand external mechanical forces and maintain thermal stability of hair [20].

The greatest drawback of pure hair protein films was brittleness, which led to poor handling and limited accessibility [3]. Hence, plasticizers were used to increase flexibility. However, the plasticizers might cause some undesirable outcomes due to leaching or crystallization during long term storage [21]. In this study, a novel keratin film was fabricated by using purified keratins alone. To the best of our knowledge, this is the first study where a plasticizer-free human hair keratin-based film has been found to be flexible and easy to handle. Human epidermal keratinocytes (HEKs) cultured on these films suggested their suitability as cell delivery substrates.

2. Materials and Methods

2.1 Human Hair proteins extraction

2.1.1 Total hair protein extraction

Human hair was collected from a local hair salon. The hair was washed twice with detergents to remove impurities and then rinsed with absolute ethanol (Merck) to facilitate its drying process at room temperature. The dried hair was then soaked in a mixture of chloroform (Sigma Aldrich) and methanol (Fisher Scientific) at a ratio 2:1 overnight in a fume hood for delipidization. After the solvents were completely evaporated, the delipidized hair was cut into lengths of 1 to 2 mm with scissors. Total hair proteins (THP), the mixture of keratins and KAP, was extracted by incubating 40 g of the cut hair in 1 L of 0.125 M $Na_2S•9H_2O$ (98+%, ACS reagent, ACROS Organics) at 40 °C for 1 hour. Next, the hair residues were removed by filtration and the resultant THP solution was dialyzed against deionized water (DI water) for the next 4 days in a cellulose tubing with 10 kDa molecular weight cut-off (Thermo Scientific

SnakeSkin Dialysis Tubing) to remove the remaining Na_2S. The dialyzed THP solution was then freeze-dried to obtain THP powder and stored at -20 °C until further use.

2.1.2 Keratins and KAP extraction

Keratins and KAP were extracted from human hair through separation protocol described previously [22]. Briefly, the delipidized hair was incubated in a KAP extraction solution pH 9 Tris-HCl buffer (Sigma Aldrich), which consisted of 8 M urea (Chem-Impex), 200 mM DTT (GoldBiotechnology), and 25 % ethanol at 50 °C for 72 hours. After that, the remaining 'KAP-free' hair residues were collected and rinsed with DI water then left to air-dry prior to the subsequent keratin extraction. The extraction of keratin was conducted in a pH 8.5 Tris-HCl buffer which consisted of 5 M urea, 2.6 M thiourea (Sigma Aldrich), and 200 mM DTT at 50 °C for 24 hours. The extracted keratin solution was dialyzed against DI water in a cellulose tubing with 10 kDa molecular weight cut-off. The dialyzed keratins solution was stored at 4 °C until up to 1 week.

2.2 Sodium dodecyl sulphate polyacrylamide gel electrophoresis (SDS-PAGE)

All chemicals and equipment for gel electrophoresis were purchased from Invitrogen unless otherwise stated. The final volume of protein sample was 20 µl which consisted of 10 µl of 1 mg/ml protein sample, 3 µl of DI water, 5 µl of LDS sample buffer (4x), and 2 µl of reducing agent (10x). For the protein ladder, 5 µl of SeeBlue™ Plus2 Pre-stained protein standard was mixed with 15 µl of DI water. Next, the samples and the protein ladder were incubated at 95 °C for 10 mins and then centrifuged at 13,000 rpm for 1 min before sample loading. NuPAGE gel (4-12 %) was used at 150 V for 45 mins with MES as a running buffer to resolve the molecular weights between 3 kDa to 198 kDa. After the run was completed, the gel was rinsed with DI water for 3 times and fixed on the rocking stage with a fixation solution (40 % ethanol and 10 % acetic acid) for 10 mins. The gel was then stained with colloidal Coomassie G-250 (Bio-Rad) on the rocking stage overnight at room temperature. On the next day, the gel was destained with DI water until the background became clear.

2.3 BCA assay

The concentration of dialyzed keratins solution was quantified by Pierce™ BCA Protein Assay Kit (ThermoFisher, Cat.23227). Briefly, the dialyzed keratins solution was diluted in DI water to meet the detection range of the BCA assay (20-2000 µg/ml). A series of dilutions of a known concentration of bovine serum albumin (BSA) was used as the standard curve. The working reagent was prepared according to the instructions provided by the supplier. The samples and the standards were placed in a 96-well plate, mixed with the working reagent, and then incubated at 37 °C for 30 mins. After the incubation, the absorbance of the samples at 562 nm wavelength was measured using a plate reader (Infinite® M200).

2.4 Keratin film fabrication

Dialyzed keratins and total hair protein solutions were adjusted to 20 mg/ml and poured into the customized polydimethylsiloxane (PDMS, Slygard 184) mold and well plate at 138.5

µl/cm^2. The samples were left at room temperature until fully dried. Figure 1 (a) shows the illustration of keratin film fabrication procedure.

2.5 Field Emission Scanning Electron Microscopy (FESEM)

Morphology of keratin film was analyzed under a FESEM (JSM-6340F, JEOL Co., Tokyo, Japan). The cross-sectioned sample was obtained by breaking the samples into half after liquid nitrogen freezing. For keratin film with cells cultured on the surface, it was fixed overnight with a mixture of 4% paraformaldehyde and 1.5 % glutaraldehyde. On the next day, the sample was dehydrated through a serial concentration of ethanol (70 %, 80 %, 90 %, and 100 %) for 2-hour interval each. The sample was then stored in dry box until completely dried. Prior to imaging, the sample was sputtered with platinum at 20 mA for 40 s. For FESEM imaging, accelerating voltage and current were set at 5 kV and 12 µA, respectively.

2.6 Water contact measurement

The water contact angle was measured at room temperature using FTA32 Contact Angle and Surface Tension Analyzer (Analytical Technologies, Singapore). 6 µl of DI water was dispensed on the sample surface at 5 µl/s.

2.7 Swelling test

Keratin films were immersed in phosphate-buffered saline (PBS) at room temperature for 5 mins and 72 hours. Length and width were measured using ruler and thickness was measure based on the optical microscopy images by ImageJ. Percentage of volume change, as well as top surface and cross-sectional surface area, were quantified according to the following equations:

Total volume changes in percentage,

$$(V_t - V_o)/\ V_o \times 100\%$$

where V_t is the swollen volume measured at wet state at time t, V_o is the original volume at dry state.

Top surface and cross-sectional area changes in percentage,

$$(A_t - A_o)/\ A_o \times 100\%$$

where A_t is the swollen area measured at wet state at time t, A_o is the original area at dry state.

2.8 Circular Dichroism (CD)

Dialyzed keratins solution was prepared at 2 mg/ml and a quartz cuvette with an optical path length of 0.1 mm was used. The CD spectrum measurement was performed at 25 °C. Data were obtained on an AVIV 420 Circular Dichroism spectrometer in wavelength steps of 0.5 nm ranging from 180 to 260 nm, with an averaging time of 0.1 s over 3 scans.

2.9 Fourier-transformed infrared (FTIR) Spectroscopy

FTIR spectroscopy was carried out in attenuated total reflection (ATR) mode for keratin film. The sample was pressed against the sample stage with a single reflection diamond element. The spectrum resolution was fixed at 4 cm^{-1} and the sample was scanned in the wavenumber range between 400 and 4000 cm^{-1}. FTIR deconvolution was done using Origin software to determine the protein secondary structure. Peaks within amide I were resolved through the second derivative.

2.10 Differential Scanning Calorimetry (DSC)

DSC (TA Instruments, U.S.) was used to evaluate the thermal properties of film samples. Prior to DSC measurements, the samples were stored in a dry box overnight to remove moisture. The samples were cut into small pieces to fit into the standard aluminium DSC pan. The experiment temperature was increased from room temperature to 400 °C at 10 °C/min.

2.11 Thermogravimetric Analysis (TGA)

TGA (TA Instruments) was used to determine the decomposition temperature of the film samples. Al_2O_3 crucible was used as a sample holder and heated from room temperature to 900 °C with a heating rate of 10 °C/min in the nitrogen atmosphere.

2.12 Tensile test in dry and wet states

Mechanical Tester (MTS C42) was used to study the mechanical properties of keratin film in the dry and wet states. Keratin film was cut into a standardized dumbbell shape with 63.5 mm in total length consisting of a gage section with 9.53 mm, 3.18 mm, and 4 mm in length, width, and thickness, respectively. The keratin film was pulled upwards by a 50 N load cell with a constant speed at 5 mm/s until broken. For the tensile test conducted in wet state, Bionix EnviroBath was filled with PBS (pH 7.2) and the keratin film was equilibrated in the PBS-filled chamber for 5 mins before the test.

2.13 Permeability test

The membrane of the cell culture insert (Millicell Hanging Cell Culture Insert, PET 0.4 µm, 24-well) was removed, replaced with keratin film, and then sealed with parafilm to prevent leakage. Prior to the permeability test, the keratin film was pre-soaked in PBS. After that, 1 % of 20 kDa FITC-dextran was prepared in PBS and dropped on the center of the keratin film. In the 24-well plate, 500 µl of PBS was filled in the well at which the level just touched the bottom of the insert without overflowed. At each time point, the cell insert with keratin film was transferred to the next well, which was already filled with fresh PBS. The fluorescence of the samples was measured by using a plate reader (Infinite® M200) for the excitation and emission wavelengths at 490 nm and 520 nm, respectively.

2.14 Cell culture

Human epidermis keratinocytes (HEKs, ATCC PCS-200-010™, US) was cultured in EpiGRO™ Human Epidermal Keratinocyte Complete Medium (Cat. #SCMK001, Millipore, US). The media were refreshed every 2-3 days and the cells were passaged when they reached 80 % confluency. HEKs at passages 5-6 were seeded onto 24-well plates and keratin film at a seeding density of 4500 cells/sample.

2.15 Sterilization of keratin film and keratin coated surfaces

Keratin films were sterilized under UV for 10 mins for each side followed by 70 % ethanol for 30 seconds. Keratin coated surfaces were sterilized under UV for 20 mins and rinsed with 70 % ethanol for 30 seconds. Sterilized keratin films and keratin coated surfaces were incubated in cell culture media for 1 day (at least two changes of cell culture media) before seeding.

2.16 Proliferation assay (PicoGreen assay)

Cell lysis was carried out by two freeze-thaw cycles of 20 min each in a cell lysis buffer (Cat. 9803S, Cell Signaling Technology, US). Subsequently, the cell lysates were mixed with PicoGreen (Molecular Probes®, US) working solution at a 1:1 ratio. All samples were incubated for 5 min at room temperature before fluorescence measurement with a plate reader (Infinite® M200) at excitation and emission wavelengths at 480 nm and 520 nm, respectively.

2.17 Metabolic assay (Alamar Blue assay)

The cells were refreshed with culture media mixed with Alamar blue reagent (Thermo Scientific, US) at 10:1 ratio followed by 2 hours incubation at 37 ºC, 95 % humidity and 5 % CO_2. The samples were then measured with a plate reader (Infinite® M200) for absorbance at the wavelengths of 570 nm and 600 nm upon colour change observed.

2.18 IL-1α ELISA

Human Interleukin 1α (IL-1α) ELISA Kit (Abcam, ab46028) was used to investigate the IL-1α secreted by HEKs cultured on keratin sample. On day 3 and day 5, the cell culture medium was removed, followed by 3 times washing with cold PBS. The cell lysate was obtained by incubating the cells in cell lysis buffer (Cat. 9803 S, Cell Signaling Technology, US) for two freeze-thaw cycles of 20 mins each. The cell lysate was used for the ELISA and stored in -80 ºC freezer for further use. All the ELISA protocol and reagents were prepared according to the instructions provided by the supplier. The absorbance of the samples at 450 nm wavelength was measured using a plate reader (Infinite® M200).

2.19 Immunoperoxidase staining

The samples were washed with cold PBS twice followed by fixation in 4% paraformaldehyde (Sigma, US) for 30 mins at room temperature. Subsequently, three-time washing with 0.05 %

Tween 20 in PBS (PBST) for 5 mins each and endogenous peroxidase quenching with Dako Real™ Peroxidase-Blocking solution (Agilent Technologies, US) for 30 mins at room temperature were performed. 10 % goat serum in PBS was then applied as a blocking solution for 1 hour at room temperature. The primary antibody against human cytokeratin 14 at 1: 200 dilution (MAB3164, Mouse monoclonal; R&D Systems) was incubated with the samples in the blocking solution overnight at 4 °C. Subsequently, secondary antibodies (EnVision™+/HRP, anti-mouse, Agilent Technologies, US) was applied onto the samples for 30 mins at room temperature, followed by DAB^+ (Agilent Technologies, US) substrate development for 30 s – 2 mins. The reaction with DAB^+ was stopped by pipetting tap water into the well once a brown colour was observed. Images were taken under an Olympus IX53 optical microscope.

2.20 Statistical analysis

All statistical analyses were done using the Origin software. Means comparison was carried out using one-way analysis of variance (ANOVA) followed by Tukey's post hoc testing, where $p < 0.05$ was considered statistically significant. All samples were run in triplicates, with three measurements taken from each sample to obtain the mean value. For swelling test, mean values were calculated with at least ten measurements from each sample.

3 Results and Discussions

3.1 Human hair protein extraction

FESEM and SDS-PAGE were done to characterize the successful extraction and separation of keratins and KAP. Based on the SDS-PAGE results from Figure 1 (b), the KAP fraction showed four bands between 6 kDa and 28 kDa which tallied with the reported molecular weight distribution of KAP [23]. On the other hand, the keratins fraction showed three visible bands at around 98 kDa, 55 kDa, and 45 kDa which represented dimers, basic, and acidic keratins, respectively. FESEM was done to observe the morphology of human hair before extraction (delipidized hair) and hair residues after KAP and keratin extraction steps, as shown in Figure 1 (c-e). Not surprisingly, only filamentous bundles, likely of the keratin intermediate filaments, could be observed after KAP removal. The FESEM images of the residues after keratin extraction showed no intact hair structures other than some fibrous remnants.

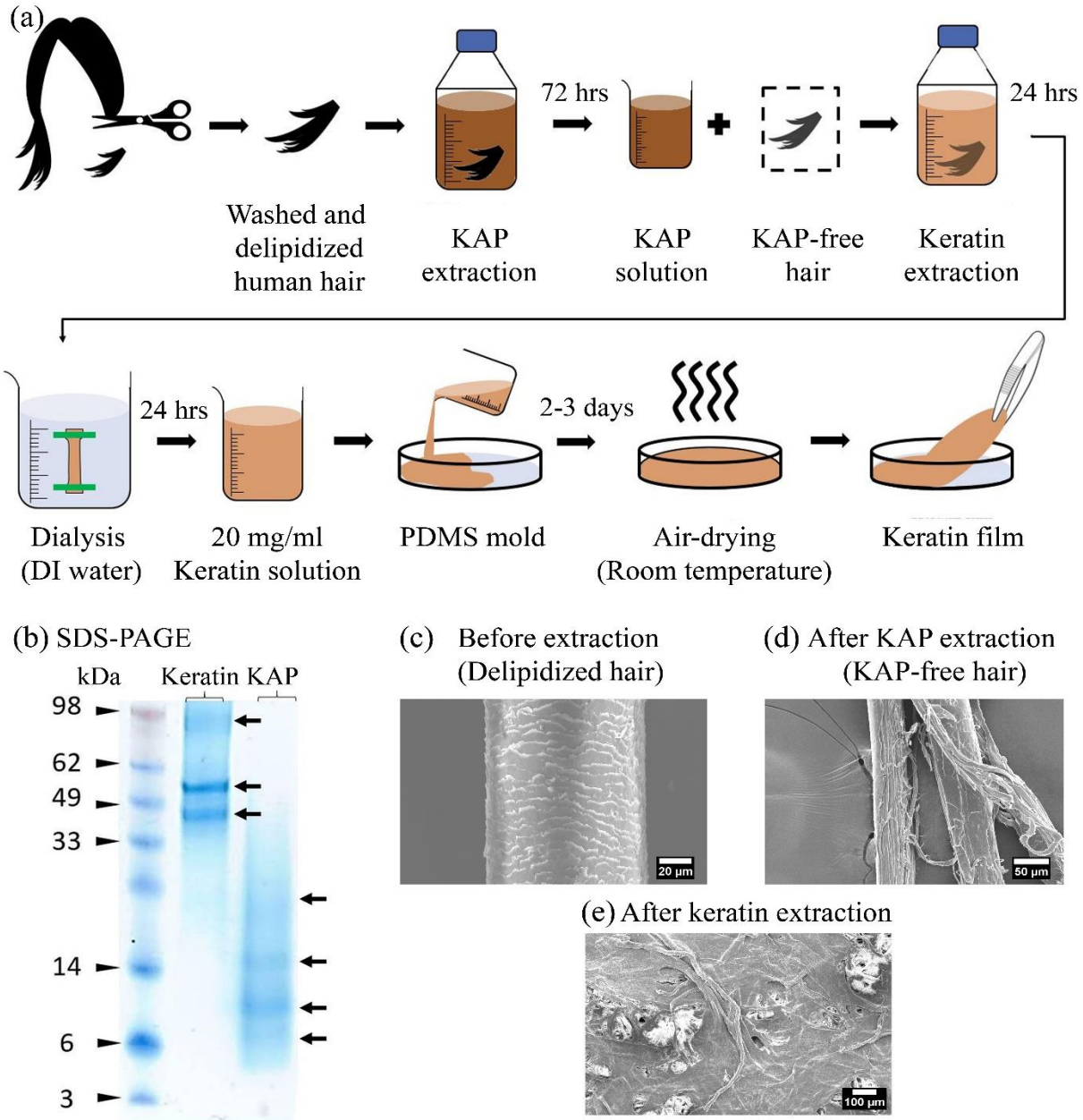

Figure 1 The evaluation of the extracted hair proteins and the schematic of the keratin film fabrication process. (a) The schematic of keratin film fabrication process. (b) SDS-PAGE results of the extracted keratins and KAP fractions. (c-e) The FESEM images of hair structures before and after extraction.

3.2 Surface characterization

The cross-section and surface morphologies of the keratin film were characterized by FESEM, as shown in Figure 2 (a-d) while a digital photograph shows the overall appearance of a keratin film (Figure 2 e). The keratin films showed porous and sheet-like cross-sectional structures with dispersed granular particles, while the top surface was smooth with no visible pore observed. Some spherical groves were found on the film surface which might be the granular particles observed in the cross-sectional images (Figure 2 c & d), which are the melanosomes in hair [24]. Interestingly, distinct and significant structures were observed across the surface

and cross-sectional images. This finding implies that the keratin film could have exhibited large-scale molecular re-arrangement during the drying process.

The sheet-like cross-sectional structures of the keratin films are very different compared to those reported in previous studies. Although these other studies used similar methods of keratin extraction, there are differences in the extraction cocktails used, which could have resulted in the differences observed. For instance, the extracted keratin solution was dialyzed against NaOH before film fabrication in Reichl et al [25]. NaOH is a strong reducing agent, which could degrade the native structure of the extracted keratins through hydrolysis in the highly basic environment, resulting in a film made up of short chain polypeptides that restrict intermolecular chain movement, hence the solid and non-porous cross-sectional structure of the film. Another study used a mixture of keratins and KAPs [26]. KAPs, which act as short linker proteins in the hair matrix, are likely to interact and form a rigid network with keratins through disulfide crosslinking, leading to a homogenous and dense cross-sectional structure. Although the films in all the studies described were fabricated from human hair proteins, the compositions of the protein mixtures are different. While only subtle differences are observed in terms of film morphology, clear differences resulting from composition differences were recorded in terms of mechanical properties, which are superior in the films reported herein.

Static water contact angles were used to characterize the surface hydrophilicity of the keratin film. Films made from THP were characterized as controls, which were referred to as THP films in the following discussions. According to Figure 2 (f & g), the water contact angle of keratin film was 88 °± 4 ° while THP film was 68 ° ± 1 °. The water contact angle of keratin films was significantly higher than that on the THP films, indicating that the keratin film surface was more hydrophobic. The hydrophobicity of keratin film surface could be due to the smooth surface structure which generally exhibited low water retention ability. In addition, the unfolded hydrophobic residues exposed on the film surfaces during the air-drying process would result in a more hydrophobic surface.

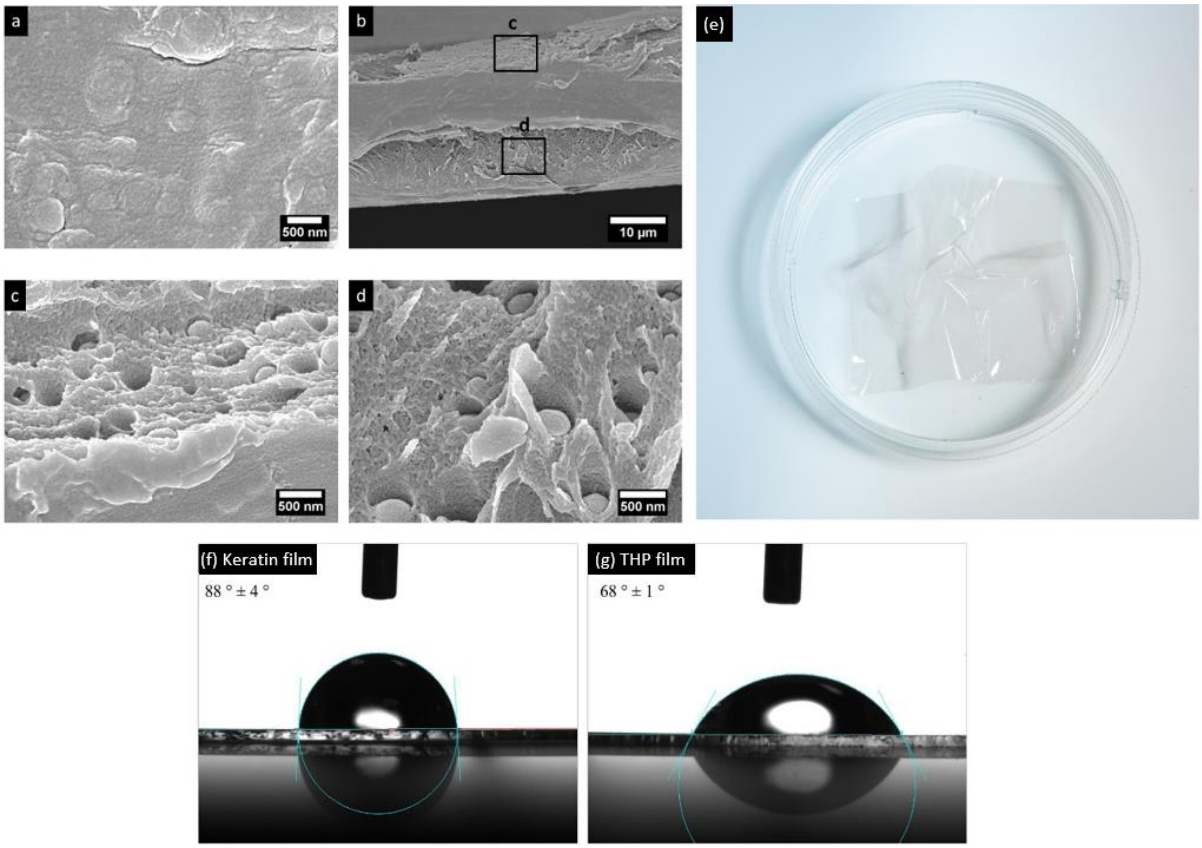

Figure 2 FESEM images of the keratin film and the results of surface wettability and swelling test. The FESEM images of keratin film: (a) surface morphology; (b-d) cross-sectional morphology; (e) digital photograph of a keratin film. The water contact angle measurements of: (f) keratin film; (g) THP film.

3.3 Swelling test

According to Figure 3 (a), the percentage change in the total volume of keratin films was not significantly changed after immersing in PBS for 5 mins and 72 hours. Regardless, the percentage change in the top surface and cross-sectional areas were quantified and compared, as shown in Figure 3 (b), with results showing that the percentage change in the cross-sectional area was significantly higher than the percentage change in the top surface area. This suggests that the swelling of the keratin film was directional, affecting the vertical axis, i.e., thickness, most significantly.

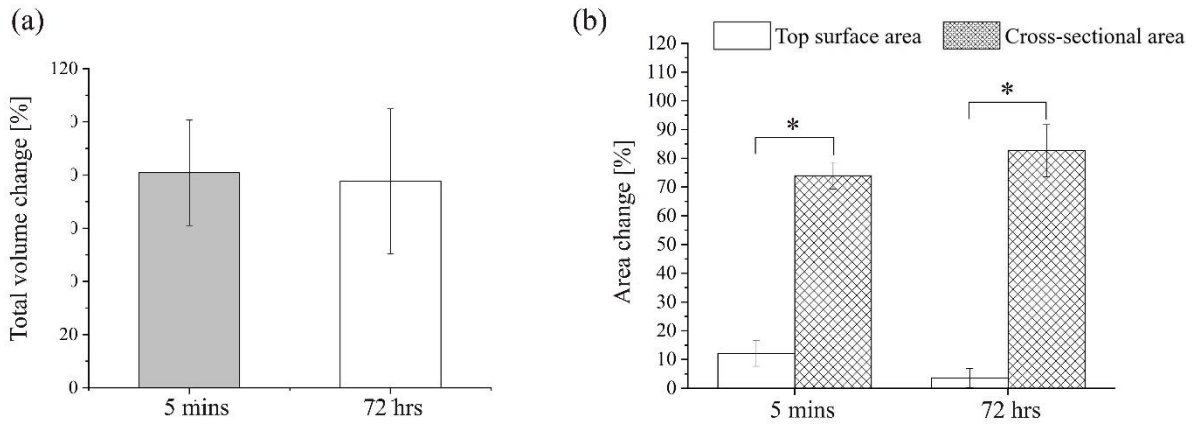

Figure 3 Swelling test results. (a) Total volume change over time. (b) Comparison of area change in percentage between top surface area and cross-sectional area over time.

3.4 Protein Secondary Structure

In this study, CD was used to determine the protein secondary structures of solubilized keratins, which represented the state before film casting. According to the CD spectrum shown in Figure 4 (a), one positive band at around 190 nm and two negative bands between 210 nm and 230 nm were recorded, representing the characteristic profile of α-helical proteins [27]. In addition, the ratio of peak intensities at 222 nm and 208 nm ($\theta_{222}/\theta_{208}$) is an indication of the likelihood of the helical structure being isolated or formed into a coiled-coil structure [28-30]. In this case, the $\theta_{222}/\theta_{208}$ ratio was approximately 1 which indicates that the coiled-coil structure was preserved. Maintaining this structure after extraction is essential for the subsequent self-assembly process [10].

The protein secondary structure of keratin film was analysed based on the deconvolution of amine I peaks from the FTIR spectral (Figure S1 in supplemental materials). The ratio percentage of each secondary structure was obtained from the area under the corresponding deconvoluted peak as shown in Figure 4 (b). The amide I deconvoluted peaks and secondary derivative of THP film and keratin film were shown in Figure 4 (c) and (d), respectively. In the keratin film, β-sheets were dominant, followed by random coils and β-turns. THP films consisted of a higher β-sheet proportion compared to the keratin films. Transition from α to β phase has been suggested as a universal mechanism of filamentous α-helical proteins exhibiting advanced mechanical properties [31]. Comparing our CD and FTIR deconvolution results, most of the helical proteins in the keratins have transformed into β-sheet, β-turn, and random coil during the film formation process. This is supported by the presence of 3_{10} helices which are the intermediates during the transition between helical and non-helical states. Changes in protein conformations are affected by a few factors, such as mechanical stress, solvent, heat treatment, freezing temperature, and freezing duration. In this study, the air-drying process provided sufficient time for molecular rearrangement which may have affected the mechanical properties. Tamada *et al.* reported the effects of drying methods on protein secondary structure transformation by manipulating freezing and drying temperatures. Self-aggregated fragments were partially transformed into β-sheets from random coils during silk-based sponge formation by the freeze-drying method [32]. Taken collectively, the differences in α-helical composition

between the solubilized keratins and cast films suggest that the transformation of protein conformation occurred during the drying process.

3.5 Thermal properties

DSC was used to study the thermal properties of keratin film. In Figure 4 (e), the water evaporation heat transfer peak was observed for both keratin and THP films within the range between 80 °C and 120 °C. Similarly, the second endothermic heat transfer of both samples occurred at around 230 °C. This peak represented the denaturation of helical protein while the enthalpy acted as the measurement of fiber crystallinity [33]. Lastly, the broad endothermic peak observed in the THP films at around 325 °C was due to β-sheet denaturation. As a comparison, the endothermic peak exhibited by keratin film was relatively small and less pronounced, suggesting that the content of β-sheet was lower. This observation corroborated with the protein secondary structure quantification by FTIR deconvolution. Since there were no significant peak shifts observed, the DSC results indicate that the thermal stability of keratin film and THP film was comparable.

TGA thermogram was used as a complementary characterization technique to investigate the thermal stability of keratin film in terms of weight loss as a function of temperature. Figure 4 (f & g) shows the TGA thermograms of keratin and THP films. The region between 25 °C and 200 °C represented the first stage of mass loss that is attributed to water loss. The second stage of the mass reduction occurred between 200 °C and 400 °C, which is mostly associated with the degradation of proteins arising from the breaking of polypeptide backbones. The decomposition temperatures of the maximum rate of weight loss of THP and keratin films were comparable, which were registered at 321 °C and 319 °C, respectively. The decomposition temperatures corresponded to the findings in DSC results where the β-sheet denaturation occurred at around 325 °C. In addition, some minor steps were observed in the derivative thermogravimetry (DTG) curves in both samples, which may correspond to the multiplicity of protein conformations of the films.

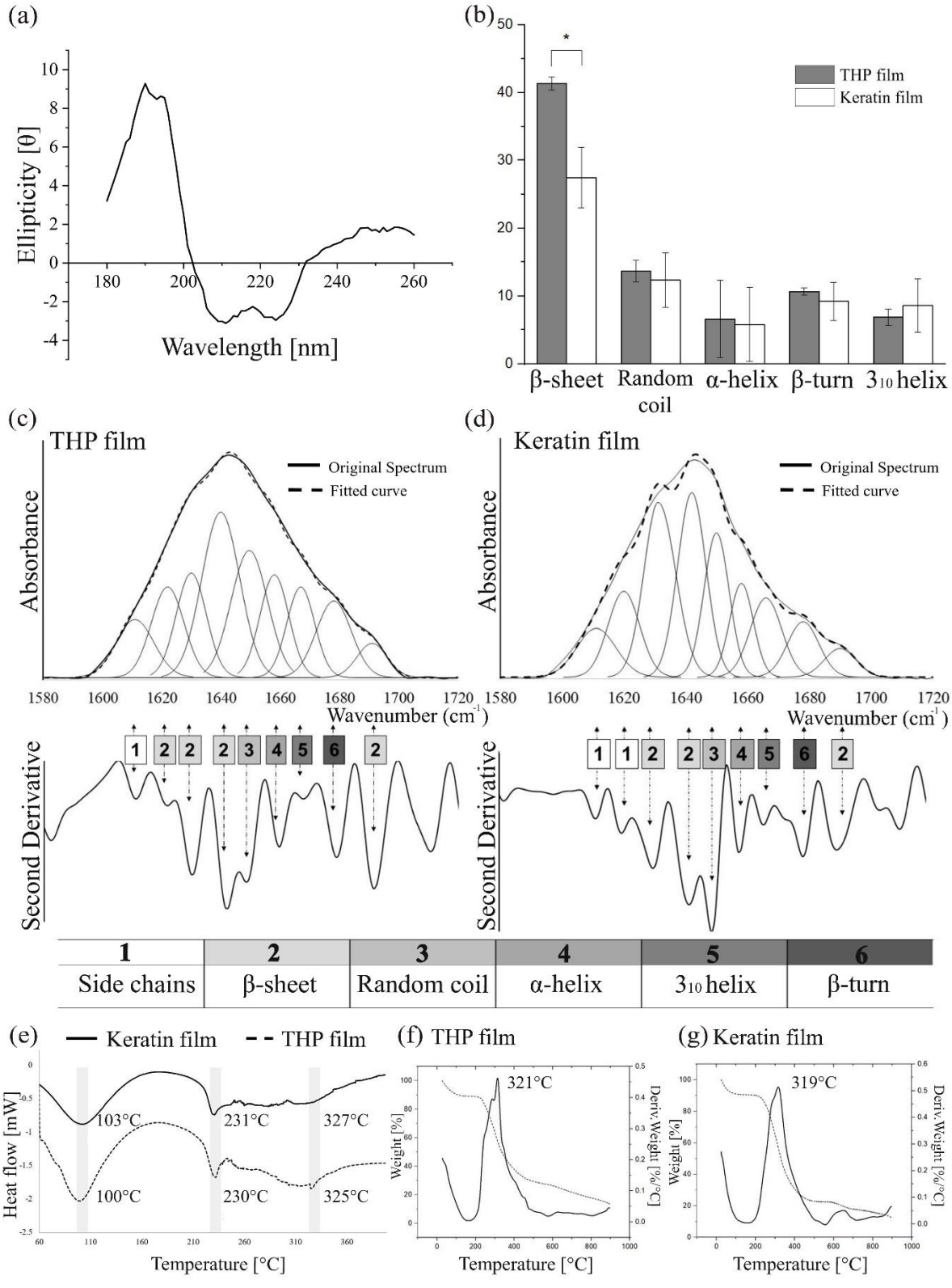

Figure 4 The protein secondary structure and thermal properties results of hair proteins films. (a) CD spectrum of keratin solution. (b) The composition percentage of protein secondary structures based on FTIR deconvoluted results. The amide I deconvoluted peaks and secondary derivation: (c) THP film; (d) keratin film. The results of thermal properties evaluation through DSC and TGA thermograms. (e) DSC spectra of keratin film (solid line) and THP film (dotted line). TGA thermograms of (f) THP film and (g) keratin film. The weight percent and the derivative weight percent are presented in dotted line and solid line, respectively. * $p < 0.05$; $n = 3$.

3.6 Tensile test in dry and wet state

Table 1 Mechanical properties of keratin film in dry and wet state.

Condition	Ultimate Tensile Strength, UTS [MPa]	Young's modulus [MPa]	Strain at break [%]
Dry	49.82 ± 6.08	1050.0 ± 90.0	6.1 ± 0.3
Wet	0.56 ± 0.18	1.0 ± 0.5	179.0 ± 17.0

The ultimate tensile strength (UTS), Young's modulus, and strain at break of keratin films in wet and dry states are summarized in Table 1 and the stress-strain curves shown in Figure 5 (a). THP films were not included because these were too fragile for the tensile tests. Results showed that keratin films exhibited UTS at 49.82 ± 6.08 and 0.56 ± 0.18 MPa in dry and wet states, respectively. The UTS of keratin films in the dry state is significantly superior to that of keratin films made with glycerol (1 MPa), keratin/chitosan blended films (27-34 MPa), and wool keratin films (20-30 MPa) reported elsewhere [34, 35]. The largest drawback of THP films was the significant brittleness which led to poor handling and limited accessibility. In contrast, our tensile test result suggests that purified hair keratins alone were capable of spontaneously crosslinking in the conditions used to form a thin film with better mechanical properties resulting in easier handling without the need for any plasticizers. The excellent mechanical property of the keratin film was found to be possible with the removal of KAP, which reduced disulfide crosslinking, allowing a less rigid molecular network to be produced. Plasticized hair protein films were found to lose the ductility and regain the brittleness when introduced into aqueous environment due to the dissolution of glycerol [34]. The keratin films in this study are made from an enriched blend of intact type I and II keratins, which promoted secondary crosslinkings that strengthen the films while allowing intermolecular sliding in the presence of long chain proteins, hence resulting in superior ductility as well. In comparison, our keratin films remained intact and even demonstrated better flexibility in wet conditions with 179 ± 17 % strain registered at the fracture point. This result proves that keratin films possessed optimal extensibility and flexibility without the presence of plasticizers and matrix proteins. It is suggested that the penetration of water molecules into the keratin films causes swelling and creates space within the structure to enable intermolecular rearrangements which contributed to the improved ductility [36]. According to Figure 5 (a), the stress-strain curve of keratin films in wet state presented a J-shape profile, which is considered as a characteristic mechanical behaviour of soft tissues [37]. The non-Hookien stress profile of keratin films in wet state also suggests secondary protein structure transition [38]. In short, this tensile test results suggest that keratin films behave differently according to the conditions: stiff and strong in the dry state; ductile and flexible in the wet state. These observations encourage further explorations to exploit these properties for meaningful applications.

3.7 Permeability

To explicate the permeability of the keratin films, permeation of 20 kDa FITC-dextran through the films was evaluated, fitted into different mathematical models and the correlation coefficients (r^2) summarized in Table S1 (supplemental materials) The permeation data was able to fit both the Higuchi and Power Law models better than the zero-order and first-order models, by showing higher correlation coefficients. The correlation coefficient of the Power Law model (0.9259) was higher than the Higuchi model (0.8667). Figure 5 (b) shows the cumulative permeability profile of 20 kDa FITC-dextran and Figure 5 (c) shows the profile fitted into the Power Law model. The results indicate that the permeability profile of keratin film follows the Power Law model and the permeation mechanism was not only dependent on diffusion, which is driven by the concentration gradient, but also associated with matrix erosion or dissolution [39]. Accordingly, the permeation mechanism can be classified by the release exponent, n, the linear regression of the graph [40]. In our study, the value of n was 0.6722, indicating that the permeability mechanism of 20 kDa FITC-dextran is specific to anomalous transport (Fickian diffusion together with matrix erosion; $0.5 < n < 1$).

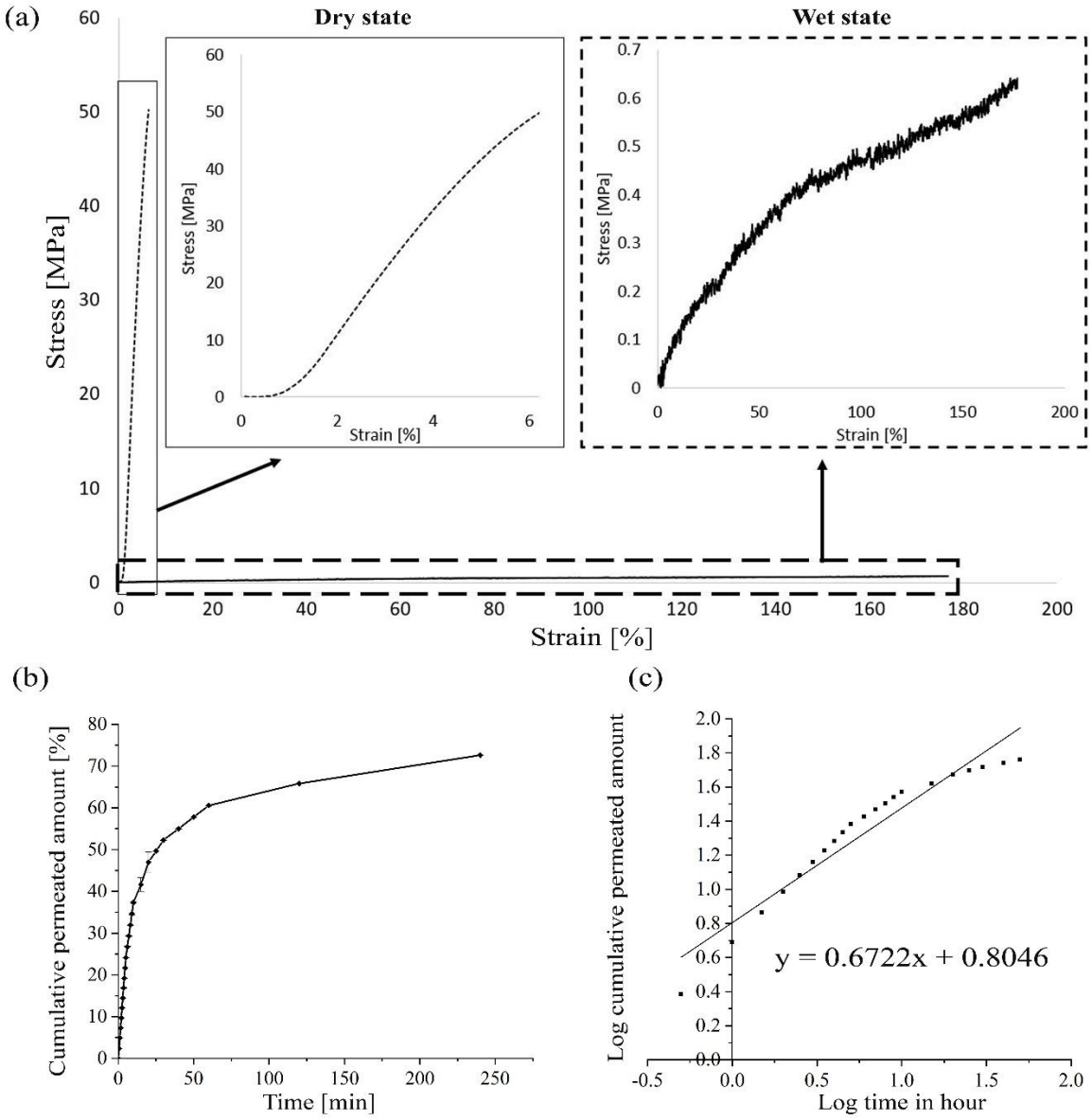

Figure 5 The tensile test and permeability test results of the keratin films. (a) Stress-strain profiles in dry state (dotted line) and wet state (solid line). (b)The cumulative permeability profile of 20 kDa FITC-dextran and (c) the curve fitted to the Power Law model.

3.8 *In vitro* results

HEKs were cultured in 24-well plates with four different surface treatments: uncoated control (tissue culture plate) and surfaces coated with 20 mg/ml keratin, 20 mg/ml THP or 2 mg/ml collagen I (positive control). The morphologies of HEKs were monitored up to day 5 as shown in Figure 6. According to the images, the colony formation and confluency of HEKs were comparable among the uncoated control, collagen I, and keratin coated samples. Consistent cell colony features of HEK on keratin sample were observed through FESEM images (Figure S3 in supplemental materials). This is supported by the presence of the LDV cell adhesion motif in keratins. In addition, Bush *et al*. revealed that positively charged and hydrophobic

surfaces provided more cell-binding sites for keratinocytes, resulting in cell adhesion and spreading [41]. Thus, the relatively low wettability might also have enhanced the affinity of HEKs to keratin films. In comparison, HEKs were barely attached to 20 mg/ml THP coated samples. THP contains both keratins and KAPs but the LDV cell adhesion motif is only present in the keratins. KAPs are the natural short linker proteins in the hair matrix, and contain a high proportion of cysteine residues, allowing efficient crosslinking with keratins through disulfide bond formation. It is postulated that the presence of KAPs in the THP samples resulted in excessive crosslinking, thereby masking a significant proportion of the LDV motifs in the keratins, rendering them inaccessible to the HEKs. It is known that HEKs perform poorly when cell densities are low, thus the cultures were unsustainable over time on THP samples.

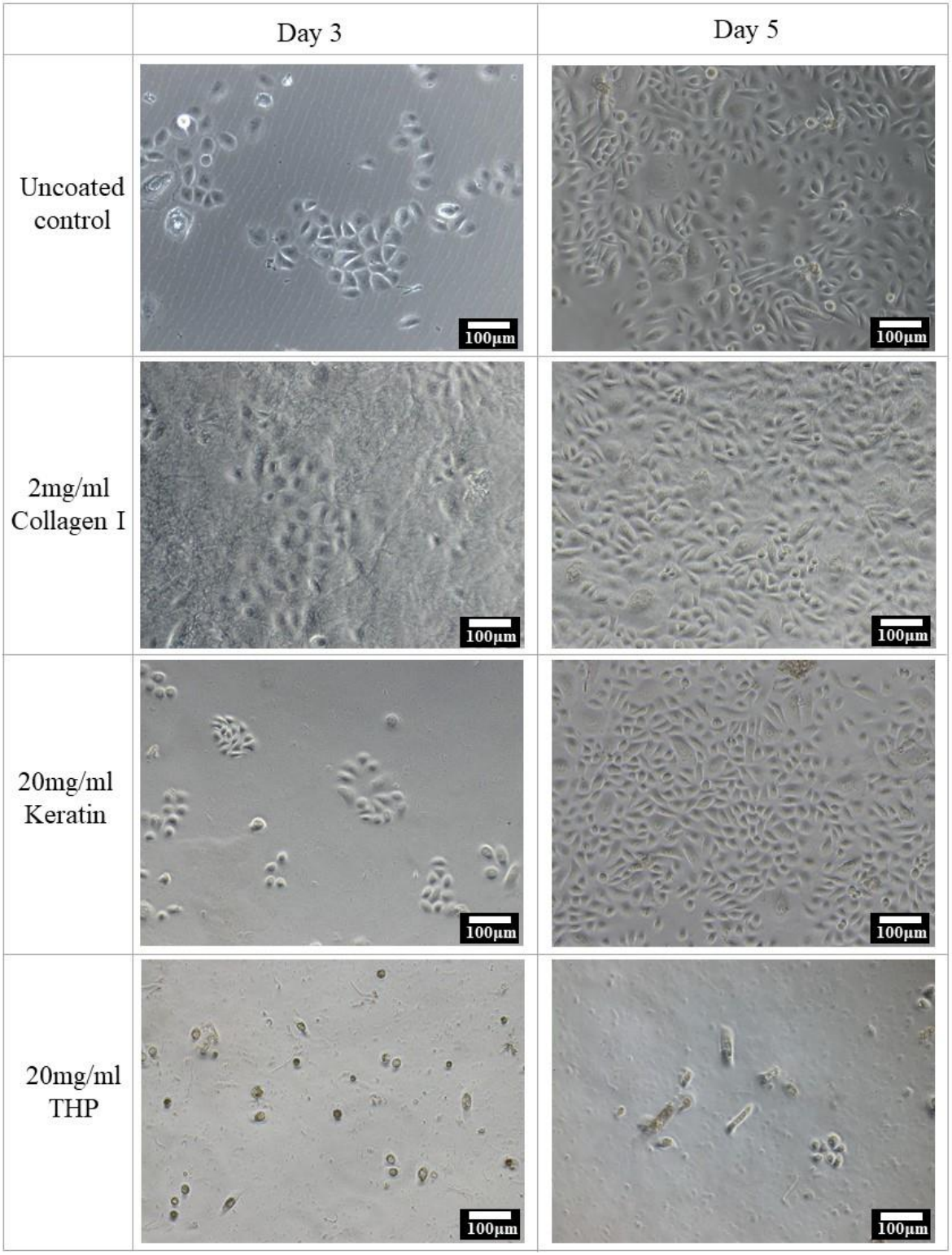

Figure 6 Phase contrast light microscopy images of HEKs cultured on various samples.

The proliferation of HEKs was quantified by the PicoGreen assay and the results are shown in Figure 7 (a). On day 3, the proliferation of HEKs was not significantly different between the uncoated control, collagen I, and keratin coated samples. However, it was significantly lower in the THP coated samples. This is mostly due to the poor cell attachment of HEKs as discussed in the previous section. Although HEK proliferation on keratin coated samples was significantly lower than on collagen I coated samples on day 5, it was comparable to the uncoated control. This is encouraging and indicates that the keratin film supports cell proliferation of HEKs.

To understand the metabolic activity of HEKs on various samples, the Alamar Blue metabolic assay results were normalized with dsDNA quantities obtained from the PicoGreen proliferation assay, as summarized in Figure 7 (b). On day 3, all samples were significantly different from each other, with cells cultured on keratin coated samples recording the highest normalized metabolic activity. On day 5, the metabolic activity of HEKs became comparable among uncoated controls, collagen I, and keratin coated samples. However, THP sample recorded significantly lower metabolic activity compared to all other samples on days 3 and 5. This result indicates that the cell growth response of HEKs cultured on keratin sample is comparable to collagen I.

The IL-1 family of cytokines are integral in the initiation and regulation of inflammatory response. Among these, IL-1α plays a major role in initiating inflammation and is released by keratinocytes. According to the ELISA results presented in Figure 7 (c), the IL-1α expression in the keratin coated samples was higher than in the uncoated controls and collagen I coated samples on days 3 and 5. This suggests that keratin as a coating might initiate inflammation in HEKs. Regardless, it is worth noting that IL-1α can promote wound healing by stimulating proliferation as well as migration of HEKs [42]. In other words, IL-1α expression in the context of this study could be exploited as a mitogen to encourage cell proliferation. The implication of this observation will need to be further investigated.

Keratin 14 (K14) is a marker of mitotically active basal keratinocytes. In this study, immunoperoxidase staining of K14 was used as a complementary characterization technique to determine the capability of keratin films in maintaining the functionality of progenitor HEKs. According to the brightfield microscopy images shown in Figure 7 (d), HEKs on keratin films showed extensive staining of K14. This implies that the keratin films could be useful substrates that allow HEKs to maintain their functional and remain highly proliferative.

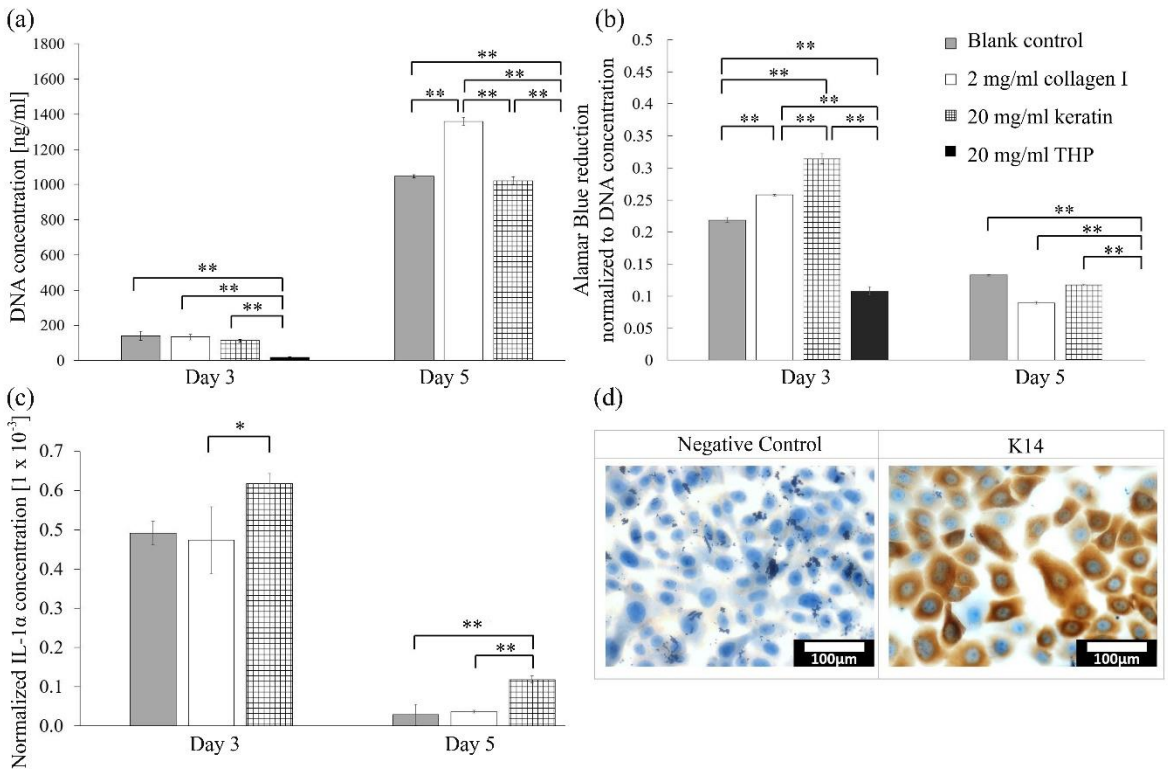

Figure 7 The evaluation results of HEK's cell responses through (a) proliferation by PicoGreen assay; (b) metabolic activity by Alamar Blue assay; (c) expression of IL-1α by ELISA and (d) immunoperoxidase staining of K14. * $p < 0.05$; ** $p < 0.01$; $n = 3$.

4 Conclusion

In this study, extracted hair keratins were successfully cast to form a film without the need for any crosslinkers or plasticizers. Uniaxial tensile tests showed that the keratin films were ductile in the dry state (Young's modulus of 1.05 ± 0.09 GPa) and viscoelastic in the wet state (179 ± 17 % strain-at-break). It is proposed that the hair keratins were capable of crosslinking spontaneously with one another in the conditions provided, and that the absence of KAPs reduced disulfide crosslinking, allowing a less rigid molecular network to be produced. *In vitro* studies showed that the keratin films offered a cell compliant surface to support adhesion, spreading, and proliferation of HEKs. In summary, our results show that a plasticizer-free film with improved mechanical properties can be fabricated by simple casting of enriched human hair keratins. The behaviour of this keratin film is unique although a longer fabrication time is required due to the need to remove KAPs before keratin harvesting. The ease of handling and cell compatible properties of the keratin film render it a potential cell carrier substrate. This work also provides a platform to further study the assembly of hair keratins to enrich current understanding of this material for development into various functional biomaterial templates.

5 Acknowledgement

This research is supported by the Agency for Science, Technology and Research (A*STAR) under its Wound Care Innovation for the Tropics, IAF-PP (H17/01/a0/0L9). The authors acknowledge the Facility for Analysis, Characterization, Testing and Simulation (FACTS), NTU, for the support in electron microscopy analysis.

References

[1] J. Hodde and M. Hiles, "Constructive soft tissue remodelling with a biologic extracellular matrix graft: overview and review of the clinical literature," *Acta chirurgica Belgica,* vol. 107, no. 6, pp. 641-547, 2007.

[2] M. Ahmad and S. Benjakul, "Extraction and characterisation of pepsin-solubilised collagen from the skin of unicorn leatherjacket (Aluterus monocerous)," *Food Chemistry,* vol. 120, no. 3, pp. 817-824, 2010.

[3] J. G. Rouse and M. E. Van Dyke, "A review of keratin-based biomaterials for biomedical applications," *Materials,* vol. 3, no. 2, pp. 999-1014, 2010.

[4] W. S. Singh V, Ng KW, "Keratin as a Biomaterial," in *Comprehensive Biomaterials II*, G. D. Ducheyne P, Healy KE, Hutmacher DW and Kirkpatrick CJ, Ed. Oxford: Elsevier, 2017, pp. 542-557.

[5] H. Lee *et al.*, "Human hair keratin and its-based biomaterials for biomedical applications," *Tissue Engineering and Regenerative Medicine,* vol. 11, no. 4, pp. 255-265, 2014.

[6] R. Fraser, T. MacRae, and G. Rogers, "Structure of α-keratin," *Nature,* vol. 183, no. 4661, pp. 592-594, 1959.

[7] R. Moll, W. W. Franke, D. L. Schiller, B. Geiger, and R. Krepler, "The catalog of human cytokeratins: patterns of expression in normal epithelia, tumors and cultured cells," *Cell,* vol. 31, no. 1, pp. 11-24, 1982.

[8] R. Moll, M. Divo, and L. Langbein, "The human keratins: biology and pathology," *Histochemistry and cell biology,* vol. 129, no. 6, p. 705, 2008.

[9] V. Verma, P. Verma, P. Ray, and A. R. Ray, "Preparation of scaffolds from human hair proteins for tissue-engineering applications," *Biomedical materials,* vol. 3, no. 2, p. 025007, 2008.

[10] H. Y. Lai *et al.*, "Self-Assembly of Solubilized Human Hair Keratins," *ACS Biomaterials Science & Engineering,* 2020.

[11] S. Wang, F. Taraballi, L. P. Tan, and K. W. Ng, "Human keratin hydrogels support fibroblast attachment and proliferation in vitro," *Cell and tissue research,* vol. 347, no. 3, pp. 795-802, 2012.

[12] S. Wang *et al.*, "Culturing fibroblasts in 3D human hair keratin hydrogels," *ACS applied materials & interfaces,* vol. 7, no. 9, pp. 5187-5198, 2015.

[13] P. Hartrianti *et al.*, "Fabrication and characterization of a novel crosslinked human keratin-alginate sponge," *Journal of tissue engineering and regenerative medicine,* vol. 11, no. 9, pp. 2590-2602, 2017.

[14] H. M. Chua, Z. Zhao, and K. W. Ng, "Cryogelation of Human Hair Keratins," *Macromolecular Rapid Communications,* vol. 41, no. 21, p. 2000254, 2020.

[15] W. T. Sow, Y. S. Lui, and K. W. Ng, "Electrospun human keratin matrices as templates for tissue regeneration," *Nanomedicine,* vol. 8, no. 4, pp. 531-541, 2013.

[16] K. Yamauchi, A. Yamauchi, T. Kusunoki, A. Kohda, and Y. Konishi, "Preparation of stable aqueous solution of keratins, and physiochemical and biodegradational properties of films," *Journal of Biomedical Materials Research Part A,* vol. 31, no. 4, pp. 439-444, 1996.

[17] S. Reichl, "Films based on human hair keratin as substrates for cell culture and tissue engineering," *Biomaterials,* vol. 30, no. 36, pp. 6854-66, 2009.

[18] F. Taraballi *et al.*, "Understanding the nano-topography changes and cellular influences resulting from the surface adsorption of human hair keratins," *Advanced healthcare materials,* vol. 1, no. 4, pp. 513-519, 2012.

[19] B. Y. Tan, L. T. Nguyen, H. S. Kim, J. H. Kim, and K. W. Ng, "Cultivation of human dermal fibroblasts and epidermal keratinocytes on keratin-coated silica bead substrates," *Journal of Biomedical Materials Research Part A,* vol. 105, no. 10, pp. 2789-2798, 2017.

[20] D. Istrate, C. Popescu, M. E. Rafik, and M. Möller, "The effect of pH on the thermal stability of fibrous hard alpha-keratins," *Polymer degradation and stability,* vol. 98, no. 2, pp. 542-549, 2013.

[21] L. Sakanaka, P. Sobral, and F. Menegalli, "Cross-linked gelatin biofilms mechanical and permeability properties as affected by storage conditions," in *Proceedings of III Congresso Ibero-Americano de Engenharia de Alimentos, Valência, Spain*, 2001, pp. 197-202.

[22] T. Fujii, S. Takayama, and Y. Ito, "A novel purification procedure for keratin-associated proteins and keratin from human hair," *Journal of biological macromolecules,* vol. 13, no. 3, 2013.

[23] M. A. Rogers, L. Langbein, S. Praetzel-Wunder, H. Winter, and J. Schweizer, "Human hair keratin-associated proteins (KAPs)," *International review of cytology,* vol. 251, pp. 209-263, 2006.

[24] N. Zhang *et al.*, "An Enzymatic Method for Harvesting Functional Melanosomes After Keratin Extraction–Maximizing Resource Recovery from Human Hair," 2021.

[25] S. Reichl, M. Borrelli, and G. Geerling, "Keratin films for ocular surface reconstruction," *Biomaterials,* vol. 32, no. 13, pp. 3375-3386, 2011.

[26] S. Reichl, "Films based on human hair keratin as substrates for cell culture and tissue engineering," *Biomaterials,* vol. 30, no. 36, pp. 6854-6866, 2009.

[27] N. J. Greenfield, "Using circular dichroism spectra to estimate protein secondary structure," *Nature protocols,* vol. 1, no. 6, p. 2876, 2006.

[28] S. C. Kwok and R. S. Hodges, "Stabilizing and destabilizing clusters in the hydrophobic core of long two-stranded α-helical coiled-coils," *Journal of Biological Chemistry,* vol. 279, no. 20, pp. 21576-21588, 2004.

[29] S. Lau, A. Taneja, and R. Hodges, "Synthesis of a model protein of defined secondary and quaternary structure. Effect of chain length on the stabilization and formation of two-stranded alpha-helical coiled-coils," *Journal of Biological Chemistry,* vol. 259, no. 21, pp. 13253-13261, 1984.

[30] M. C. Manning and R. W. Woody, "Theoretical CD studies of polypeptide helices: examination of important electronic and geometric factors," *Biopolymers: Original Research on Biomolecules,* vol. 31, no. 5, pp. 569-586, 1991.

[31] A. Zhmurov, O. Kononova, R. I. Litvinov, R. I. Dima, V. Barsegov, and J. W. Weisel, "Mechanical Transition from α-Helical Coiled-Coils to β-Sheets in Fibrin (ogen)," *Journal of the American Chemical Society,* vol. 134, no. 50, p. 20396, 2012.

[32] Y. Tamada, "New process to form a silk fibroin porous 3-D structure," *Biomacromolecules,* vol. 6, no. 6, pp. 3100-3106, 2005.

[33] M. Spei and R. Holzem, "Thermoanalytical determination of the relative helix content of keratins," *Colloid & Polymer Science,* vol. 267, no. 6, pp. 549-551, 1989.

[34] T. Tanabe, N. Okitsu, A. Tachibana, and K. Yamauchi, "Preparation and characterization of keratin–chitosan composite film," *Biomaterials,* vol. 23, no. 3, pp. 817-825, 2002.

[35] H. Atri, E. Bidram, and D. E. Dunstan, "Reconstituted Keratin Biomaterial with Enhanced Ductility," *Materials,* vol. 8, no. 11, pp. 7472-7485, 2015.

[36] D. S. Fudge and J. M. Gosline, "Molecular design of the α–keratin composite: Insights from a matrix–free model, hagfish slime threads," *Proceedings of the Royal Society of London. Series B: Biological Sciences,* vol. 271, no. 1536, pp. 291-299, 2004.

[37] F. Xu and T. Lu, "Skin Mechanical Behaviour," in *Introduction to Skin Biothermomechanics and Thermal Pain*: Springer, 2011, pp. 87-104.
[38] D. S. Fudge, K. H. Gardner, V. T. Forsyth, C. Riekel, and J. M. Gosline, "The mechanical properties of hydrated intermediate filaments: insights from hagfish slime threads," *Biophysical journal,* vol. 85, no. 3, pp. 2015-2027, 2003.
[39] R. W. Korsmeyer, R. Gurny, E. Doelker, P. Buri, and N. A. Peppas, "Mechanisms of solute release from porous hydrophilic polymers," *International journal of pharmaceutics,* vol. 15, no. 1, pp. 25-35, 1983.
[40] N. Peppas, "Analysis of Fickian and non-Fickian drug release from polymers," 1985.
[41] K. Bush, P. Driscoll, E. Soto, C. Lambert, W. McGimpsey, and G. Pins, "Designing tailored biomaterial surfaces to direct keratinocyte morphology, attachment, and differentiation," *Journal of Biomedical Materials Research Part A: An Official Journal of The Society for Biomaterials, The Japanese Society for Biomaterials, and The Australian Society for Biomaterials and the Korean Society for Biomaterials,* vol. 90, no. 4, pp. 999-1009, 2009.
[42] J. D. Chen, J.-C. Lapiere, D. N. Sauder, C. Peavey, and D. T. Woodley, "Interleukin-1α stimulates keratinocyte migration through an epidermal growth factor/transforming growth factor-α-independent pathway," *Journal of investigative dermatology,* vol. 104, no. 5, pp. 729-733, 1995.

Authors Biography

Bee Yi Tan

Bee Yi Tan received her B.Eng. (Hons) in Materials Engineering from the School of Materials Science and Engineering, Nanyang Technological University, Singapore, in 2016, and completed her Ph.D. in the same school in 2020. Her research focuses on developing novel hair protein-based platforms, especially coatings and films, for tissue engineering applications.

Luong T. H. Nguyen

Luong T. H. Nguyen is a Scientist in the Department of Chemical and Biomolecular Engineering at the Ohio State University (USA). She received her B.Eng degree with a gold medal in Chemical Engineering from Ho Chi Minh city University of Technology (Vietnam), and her Ph.D degree in Biomedical Engineering from National University of Singapore (Singapore). She worked as a Senior Research Fellow in Nanyang Technological University (Singapore) for three years before joining OSU. Her current research interests include polymeric and nano-sized materials for tissue regeneration and drug delivery; and microfluidic devices and biochips for cancer diagnosis, immunotherapy response prediction and viral detection.

Kee Woei Ng

Kee Woei Ng holds a M.Eng. in Mechanical Engineering and a Ph.D. in Medicine. He is currently a tenured Professor at the School of Materials Science and Engineering at Nanyang Technological University, Singapore. His research focuses on the development of sustainable material platforms for soft tissue engineering, regenerative medicine and beyond. He is particularly interested in studying and developing keratin based substrates and establishing fundamental understanding of how keratins influence cell physiology.